Analysis of integrated optics elements based on photonic crystals

I. Guryev, I.A. Sukhoivanov, S. Alejandro-Izquierdo, M. Trejo-Durán, J.M. Estudillo-Ayala,
J.A. Andrade-Lucio, and E. Alvarado-Méndez*

*Facultad de Ingeniería Mecánica, Eléctrica y Electrónica, Departamento de Electrónica, Universidad de Guanajuato,
Apartado Postal 215-A, Salamanca, Gto., 36730 México,
e-mail: ealvarad@salamanca.ugto.mx.

We present the design of a demultiplexer based on photonic crystals (PC). The control of the refractive index, periodicity, geometry and size of the structure, are very important to light propagation in PC. The demultiplexer is intended to separate pulse channels with 1.3 and 1.55 μm wavelength into wide pass band wavelength division multiplexing (WDM) optical telecommunications systems. The dependence of the band gap width on the refractive index $\triangle n$ between background and road lays is shown. The results of FDTD numerical simulation of wavelength channel splitting and the spectral analysis for the maximum efficacy of transfer energy are also presented.

Keywords: Photonic bandgap materials; devices; integrated optics.

Presentamos el diseño de un demultiplexor basado en cristales fotónicos (PC). El control del índice de refracción, periodicidad, geometría y tamaño del dispositivo, es muy importante para la propagación de la luz en un PC. El propósito de hacer un demultiplexor es separar pulsos por canales de 1.3 y 1.55 μm de longitud de onda en sistemas de comunicaciones ópticos (WDM). La dependencia del ancho de banda prohibida, respecto a la diferencia entre el índice de refracción de fondo y el de las capas formadas por los cilindros $\triangle n$, es mostrado. Los resultados de la simulación numérica FDTD del canal de longitud de onda es dividido y el análisis espectral para la eficiencia máxima de transferencia de energía es presentado.

Descriptores: Materiales de bandas fotónicas; divisores de haz; óptica integrada.

PACS: 42.70.QS; 42.79.-e; 42.82.-m

1. Introduction

At the moment, photonic crystals, structures with periodically changing refractive index, have advanced in popularity due to the possibility of controlling light distribution in IR, visible and UV ranges [1-2]. Owing to changes in the periodicity of material parameters, the photonic band gap (PBG) appears. PCs are particularly interesting, in all-optical systems to transmission and processing information due to the effect of localization of the light in the defect region of the periodic structure. Among the most important application areas of PCs are low-threshold single mode lasers (where PCs are used as the optical confinement factor), wavelength filters, optical waveguide structures, WDM system devices [3,4], splitters and combiners [5]. Wavelength filters of optical range based on the one-, two- and three-dimensional PBG structure [3], [6-8] can be created by the correct selection of geometrical and physical parameters. There are inherent limitations due to the narrow band spectrum background [9]; PC waveguides with line defects must be improved by the embedding of additional 1D or 2D PCs. Optical frequency filters, and particularly demultiplexers, can be based on one-dimensional PCs [10] in combination with optical circulators [11]. These demultiplexers consist of circulators placed one by one with precisely tuned Bragg reflectors between them. This technology makes it possible to separate frequency channels with less than 100 GHz. But due to the large size, the technology cannot be effectively used in integrated optical circuits. Wavelength channel separation produced by using an interference splitter [12] required a strong

single mode and position of output channels. The demultiplexer can also be made using the high-Q nanocavities based on 2D PCs [13,14]. However, none of these devices fulfil the requirements of high transmission bandwidth which are necessary for wide pass band WDM systems with the short pulses of demultiplexing. Devices presented in Refs. 7 and 15 for wide pass band system are based on wave coupling in the PC waveguide couplers with strong mode coupling in PC channel, but they require quite long coupling sections.

Another approach is to use a PC splitter with wavelength filters [16]. We propose the method for the integrated PC based wavelength demultiplexing system design. This device is represented by the optical waveguide channel created by introducing a line defect into the periodic structure of the 2D PC. At the output of the channel in the same structure, the 1×2 splitter is created. At the input of each port of the splitter, the wide band optical filter, formed by variation of geometrical parameters of the PC, is placed. Each filter has the precision calculated for the band gap to provide the most efficient wavelength channel splitting. In this work, band diagrams of square lattice and hexagonal lattice PCs are investigated in detail. A device for wavelength channel splitting based on wide band filters is developed, and its parameters are calculated. Also are investigated spectral characteristics of the device as well as its information properties.

2. Idea and Physical Model

As was mentioned above, the device to optical wavelength channel splitting is represented by the PC, in which condi-

tions for selective radiation distribution were created by introducing defects into the regular structure and by the variation of the elements parameters. These conditions can be found by the PBG analysis with further determination of PC parameters. An infinite, strictly periodic structure of the PC is characterized by the PBG, which depends on the ratio the of refractive index of background and rod materials, and geometric parameters of the structure. When the device is created by variation of these parameters, then the periodicity is broken. Consequently areas with the modified PBG appear. Within the framework of this study, we assume that the PBG of an infinite periodical structure does not essentially differ from a finite one. The validity of this statement is proved by numerical simulations of the characteristics of the structure and will be described below. Thus, the PBG of the finite structure can be calculated using the method for the strictly infinite periodic structure. To obtain the PBG for the periodic structure we can use the plane wave expansion method (PWE). This method provides an easy solution to the eigenvalue problem for wave Helmholtz equations (1). In this task, the stationary Helmholtz equations in the approach of non-magnetic media are used:

$$\frac{1}{\epsilon(\overrightarrow{r})}\nabla \times \{\nabla \times \overrightarrow{E}(\overrightarrow{r})\} + \frac{\omega^2}{c^2}\overrightarrow{E} = 0 \qquad (1)$$

where $\overrightarrow{E}$ is the electric field, $\overrightarrow{r}$ is the generalized coordinate, ω is the structure's eigenfrequency, c is the light velocity in a vacuum; $\varepsilon(\overrightarrow{r})$ is the permittivity profile of the structure.

In order to find eigenfrequency values for the periodic structure, it is convenient to take advantage of the Bloch theorem. According to the theorem, function $\overrightarrow{E}$ can be represented as plane waves multiplied by the periodic function with the period equal to the structure period,

$$\overrightarrow{E}(\overrightarrow{r}) = \overrightarrow{u}_{\overrightarrow{k},n}(\overrightarrow{r})e^{i*\overrightarrow{k}*\overrightarrow{r}}, \qquad (2)$$

where $\overrightarrow{u}_{\overrightarrow{k},n}(\overrightarrow{r})$ is a periodic function, $\overrightarrow{k}$ is the wave vector and n is a band number.

Functions $1/\epsilon(\overrightarrow{r})$ and $\overrightarrow{E}(\overrightarrow{r})$ can be expanded to the Fourier series by reciprocal lattice vectors:

$$\frac{1}{\epsilon(\overrightarrow{r})} = \sum_{\overrightarrow{G}} \chi(\overrightarrow{G}) * exp(i\overrightarrow{G} * \overrightarrow{r}), \qquad (3)$$

$$\overrightarrow{E}_{\overrightarrow{k},n}(\overrightarrow{r}) = \sum_{\overrightarrow{G}} \overrightarrow{E}_{\overrightarrow{k},n}(\overrightarrow{E})exp(i*(\overrightarrow{r}+\overrightarrow{G})*\overrightarrow{r}), \quad (4)$$

where $\overrightarrow{G}$ is the reciprocal lattice vector. Substituting (4) into (1), we obtain a linear equation set with unknown $\omega_{\overrightarrow{k},n}$ eigenfrequency in the $\overrightarrow{k}$-th point of the n-th band:

$$-\sum_{\overrightarrow{G'}} \chi(\overrightarrow{G}-\overrightarrow{G'})(\overrightarrow{k}+\overrightarrow{G}) \times \{(\overrightarrow{k}+\overrightarrow{G'}) \times \overrightarrow{E}_{\overrightarrow{k},n}(\overrightarrow{G'})\}$$

$$= \frac{\omega_{\overrightarrow{k},n}}{c^2}\overrightarrow{E}_{\overrightarrow{k},n}(\overrightarrow{G}). \qquad (5)$$
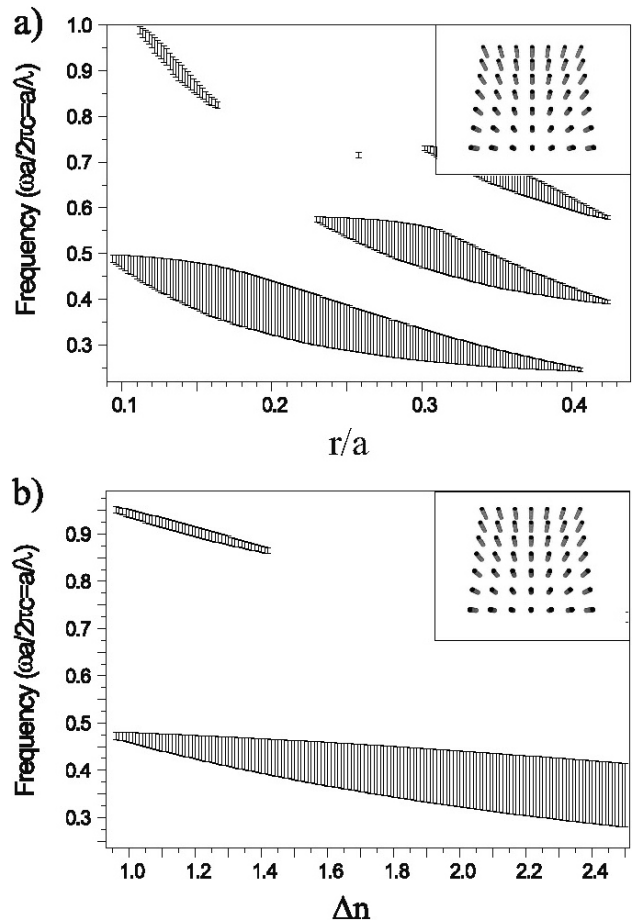

FIGURE 1. TM Band-gap maps of the square lattice PC by different radius-to-pitch ratio (a), and by the difference in the refractive indices of rod and background materials (b).

Solving Eq. (5) numerically for each point of reciprocal lattice space in the first Brillouin zone, we can obtain the PC band structure. Band gap maps calculated for TM polarization of light propagated in two dimensional PC consisting of square lattice parallel rods are plotted in Fig. 1. In this work we consider TM polarization because PC is formed by a rod structure and is characterized by a wider band gap area with TE polarization [17].

In Fig. 1a the dependence of the band gap width *vs.* placement on the normalized rod radius r/a, is shown. Here, the relative frequency means the angular frequency normalized by the distance between rod centers (pitch):

$$\omega_r = \frac{\omega a}{2\pi c} = \frac{a}{\lambda} \qquad (6)$$

Constant parameter values are: background refractive index $n_1 = 1$, rod refractive index $n_2 = 3$, and pitch $a = 0.55\ \mu m$. The value of the rod radius divided by pitch varies in the range of 0.1 - 0.5. As is seen from Fig. 1a, the lowest band gap is the longest one. While the rod radius increases, the band gap frequencies decrease and the PBG width changes. Moreover, the widest band gap is observed in the area where the ratio of the rod radius divided by is pitch equal to 0.2.

In Fig. 1b is shown the dependence of band gap width and placement on the difference between the background and rod refractive index $\triangle n = n_2 - n_1$. In this case, constant parameters of the structure are: background refractive index $n_1 = 1$, pitch $a = 0.55$ μm, and the value of the rod radius divided by pitch is equals to 0.1. As is seen from Fig. 1a, the lowest band gap is the widest and longest one. The band gap width increases monotonically with the growth of the difference in indices. At the same time, the central frequency of the band gap decreases.

Fig. 1 shows that it is possible to control the behavior of the PBG when changes the rod radius or refractive index difference between rod and background materials changes. From the technological point of view, it is easier to fabricate structures with a variation in geometric parameters than a variation in the refractive index. Moreover, in the case of a variation in geometric parameters, the central band gap frequency can be changed in the range of 0.25 - 0.48; and in the case of a variation in the difference of refractive index, which is typical for semiconductor-air structures, this range is 0.35 - 0.47. The upper edge of the band gap, changes much more slowly than the lower edge (see Fig. 1b). These facts complicate the task when we work with the variation in refractive index.

3. Demultiplexer on the Base 2D PC

To specify the main parameters of the device, it is necessary to determine the exact difference between refractive index and geometric parameters of the PC waveguide channel and PC filters. For this reason, let us consider the band gap width and placement dependence on the rod radius divided by the pitch value (Fig. 2). For the largest band gap parameter variation, it is useful to work with the lowest band gap (Fig. 1).

In Fig. 2 horizontal solid lines indicate channels of normalized frequencies ω_{r1} and ω_{r2}, while vertical solid lines indicate rod radius for the first filter r_1, main waveguide
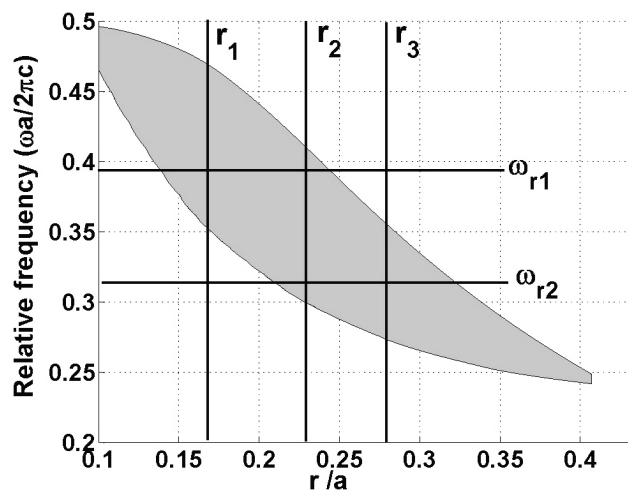

FIGURE 2. The scheme for selection of geometric parameters using band-gap map.

channel r_2, and the second filter r_3. Figure 2 shows that the PC with rod radius r_2 has the band gap that permits the reflectance for both frequency channels, and a longitudinal defect in this PC will form the waveguide channel and splitter. At the same time, PCs with rod radius r_1 and r_3 have the band gap only for one of two frequency channels. The PCs with these parameters form frequency filters. Thus we have relative frequency on the ordinate axis, and it is possible to select any relation of channel wavelengths. In particular, in this paper we shall investigate the demultiplexer for channels with wavelengths of 1.55 and 1.31 μm.

The selection process of structure parameters consists of several steps. Firstly, it is necessary to determine one of two relative frequencies ω_r. From the relative frequency and channel wavelength the pitch value for PC of the first filter can be obtained from Eq. (6), and then the relative frequency of the second channel can be found. The frequencies obtained must satisfy the condition for the existence of the rod radius value (Fig. 2), at which both frequencies are within the band gap of the basis PC structure. This task can be simplified with its preliminary graphical solution indicated in Fig. 2.

Finally, we have a PC structure with the following parameters for the square lattice: the background refractive index $n_1 = 1$, rod refractive index $n_r = 3$, distance between rod centers $a = 0.55$ μm, $r_1 = 0.108a$, $r_2 = 0.175a$, and $r_3 = 0.229a$. The structure parameters for the device with hexagonal PC lattice are: background refractive index $n_1 = 1$, rod refractive index $n_r = 3$, distance between rod centers, $a = 0.65$ μm, $r_1 = 0.11a$, $r_2 = 0.17a$, and $r_3 = 0.235a$.

As a result based on the method of PBG, parameters of the demultiplexer have been selected. This method does not give any information about behavior structure outside of PBG, and cannot give an optimal solution, which demand the additional investigation into spectral characteristics by reasonable alteration of geometrical parameters. Thereupon we present a spectral analysis (the spectral dependence of the power on each output port of the device) and data (maximum available bit rate determined by the frequency filter properties) characteristics.

4. Numerical Results

We propose a two-channel wavelength division demultiplexer, represented by the integrated device based on the c square or hexagonal lattice 2D PC, for 1.55 μm and 1.31 μm wavelength channels of separation, respectively.

Wavelength demultiplexing is carried out using a 2-channel splitter, and the elements are indicated in Fig. 3. In general, square and hexagonal devices have a similar design and only in the form of output splitter channels. Demultiplexer consists of input channel (In) produced by the W1 waveguide made of a line defect formed by removing one row of rods from the background PC. This waveguide connects to the splitter with two output ports SO1 and SO2. We propose to set in the output ports of the splitter, the wide band
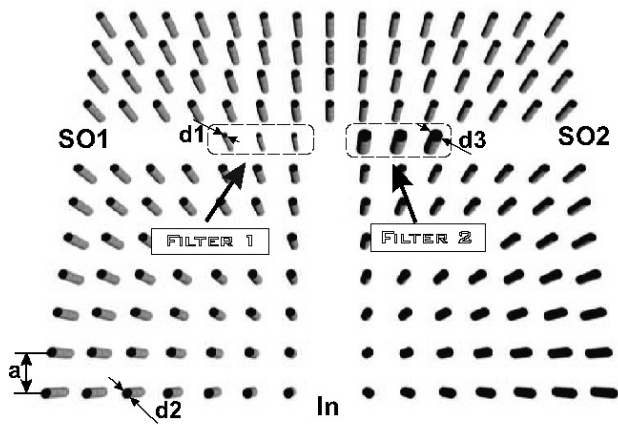
a) T-splitter
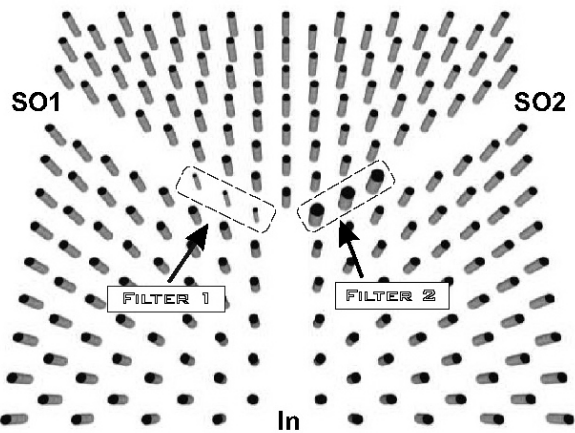
b) Y-splitter

FIGURE 3. Diagram of the optical demultiplexer based on a PC splitter with the square (a) and hexagonal (b) lattice. Rod diameters d1, d2 and d3 correspond to elements of filter 1, background PC with pitch a, and filter 2 respectively.

frequency filters, created by three successive rods with diameters d_1 and d_3. As we have seen in Fig. 3, the filters embedded in the output waveguides have the same lattice constant and are placed in accordance with the lattice of background PC. Moreover, we present results for the modified square lattice device. Its main input waveguide has a specific peculiarity, which consists in the continuity of the input waveguide beyond the bound of T-shaped splitter (Fig. 3a) and the creation of the continuous W1 waveguide. This fact does not affect the efficiency of demultiplexing, but it makes it possible to decrease the reflectivity of the whole structure at the operating wavelengths more than 3 times. This is illustrated in Fig. 4. On the other hand, the continuity structure provides a higher data transfer rate because of avoiding the parasitic resonances at the point of the channel splitting.

The investigation into of the characteristics of this demultiplexer was conducted on the basis of a numerical experiment using the finite difference method in time domain
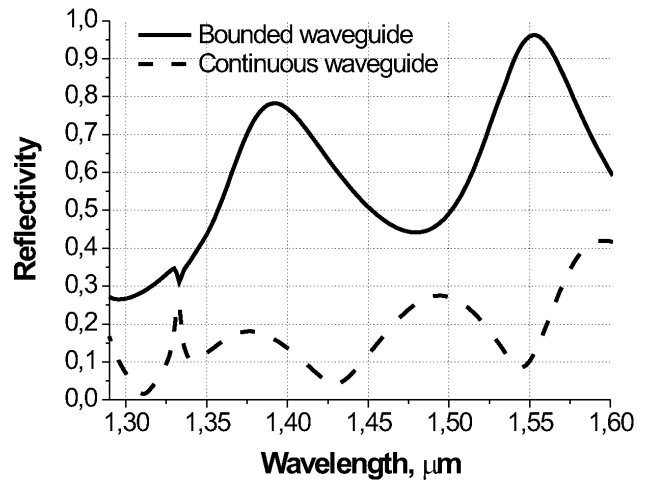

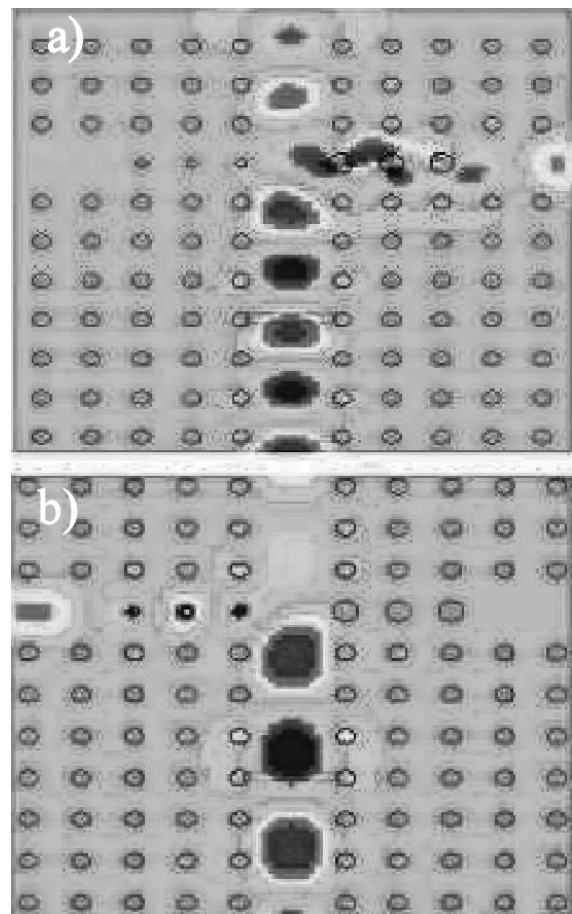FIGURE 4. Reflectance from the splitter for bounded (T-splitter) and continues waveguides (X-splitter).

FIGURE 5. Results of FDTD simulation of wavelength channel splitting for (a) source wavelength $1.31\mu m$, and (b) source wavelength $1.55\mu m$.

(FDTD) [18-20]. Computed electromagnetic field distribution in the square lattice PC demultiplexer is shown in Fig. 5 for two transmitted signals with wavelength 1.31 μm (Fig. 5a) and 1.55 μm (Fig. 5b). Filter 1 with $r_1 < r_2$ in the left channel of the splitter fully reflects the radiation with

wavelength 1.31 μm, and filter 2 with $r_3 > r_2$ in the right channel reflects the radiation with wavelength 1.55 μm.

The analysis of the device efficiency was investigated using spectral characteristics based on square and hexagonal lattices (see Fig. 6). These characteristics were obtained by computer calculate for each wavelength.

In case of the square lattice PC the reflectance is almost absent; however, the power distribution for each channel is not uniform. Transmission for the channel 1.55 μm is twice as good as the 1.31 μm channel. For the device based on the hexagonal lattice PC, the situation is inverse: the power distributes between channels is uniform, but at the operating wavelengths the reflectance is observed. The high level of the reflectivity can be explained by low waveguide properties of the channel in comparison with devices based on cubic lattice PC.

Due to non-ideality of the filters in the secondary waveguides, parasitic penetration of the radiation of different wavelengths through the filters into the adjacent secondary waveguide, is observed. The channel separation efficiency of the device on the PCs with different lattices also can be analyzed by the dependence $P_{12} = 10 lg[P_1/P_2]$, where P_1 and P_2 are

the power at the specified wavelength on the output channel SO_1 and SO_2, respectively (Fig. 7). We concluded that the ratio of powers in the square lattice case is about 20 dB in
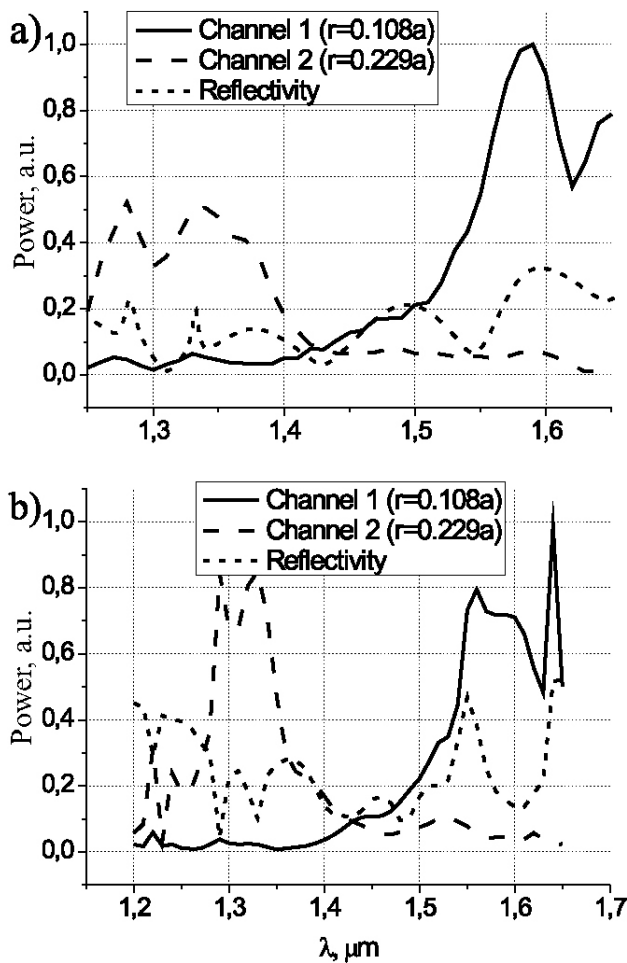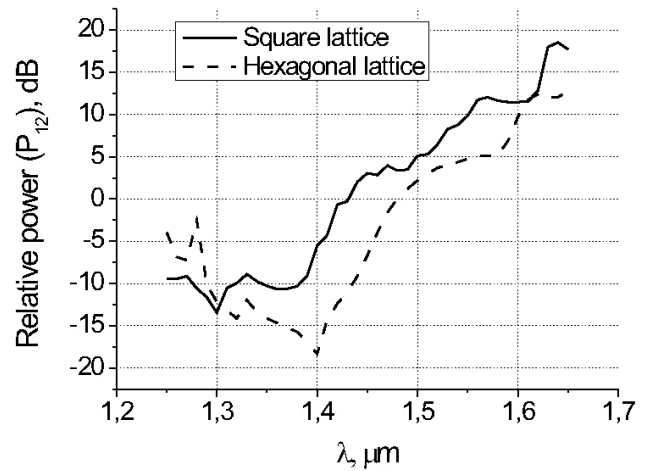
FIGURE 7. Channel power ratios for demultiplexer based on square (solid) and hexagonal (dashed) lattice PCs.
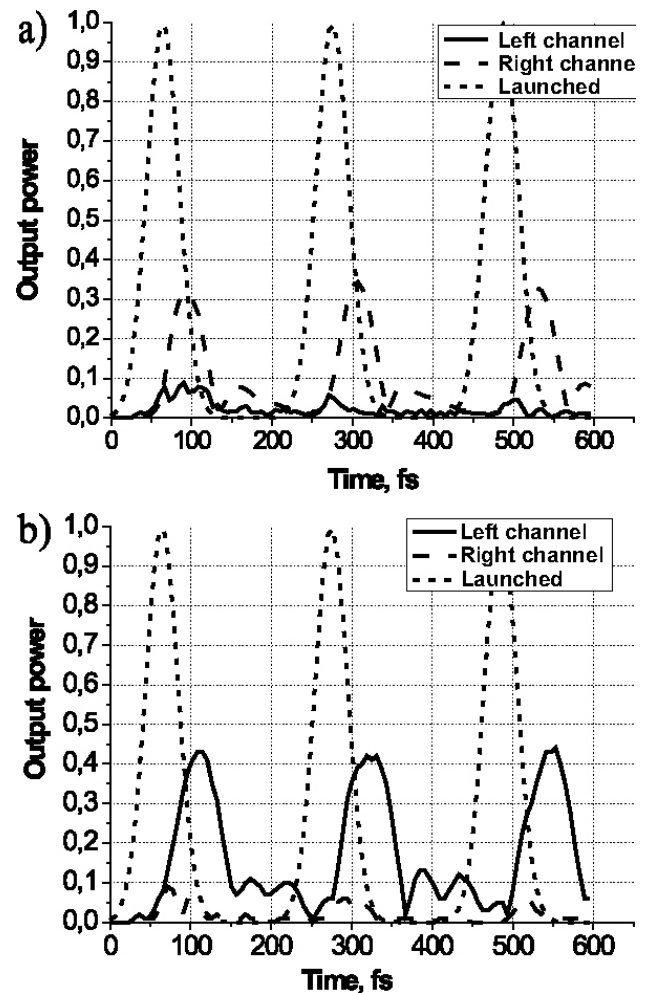
FIGURE 8. The pulse pattern responses of the demultiplexer based on the square lattice PC. (a) - source wavelength 1.31μm; (b) - source wavelength 1.55μm.

FIGURE 6. Transmission characteristics of the demultiplexer based on square lattice (a), and hexagonal lattice (b) PC.

both output channels, and the wavelengths of the system show a high separation efficiency of the demultiplexer.

One of the most significant characteristics of the integrated devices is the data transmission. To show the design of a two-channel demultiplexer, pulse pattern responses with a Gaussian pulse series of 50 fs. were studied. Pulse pattern responses of the demultiplexer based on the square lattice PC at different wavelengths are shown in Fig. 8.

We found that the attenuation of the transmitted pulse is approximately $(60 - 70)\%$, but the broadening is almost absent. Output pulses have a duration of 52 fs and 58 fs corresponding to 1.31 μm and 1.55 μm, respectively. This broadening pulse takes place by the interference of the wave in the filters, but it does not have an influence on the bit error rate because it is negligible in comparison with time interval between pulses. So pulses remain clear enough to be recovered successfully. The pulse pattern response for the demultiplexer based on the hexagonal lattice PC is similar to the square lattice PC. In both cases the low broadening is achieved by applying wide band frequency filters, and can be recommended for demultiplexing of ultrashort pulses with a very broad spectrum.

5. Conclusion

In this work we have investigated properties of the PCs based on the selection of structure parameters. The plane wave expansion method was applied to finite periodic structures. The new design of the wavelength division demultiplexer based on the integrated PCs was also proposed. The operation principles of the devices were considered and proved. Besides, the spectral and data characteristics were investigated. Due to quite satisfactory data characteristics, the device can be effectively used in novel ultra-short pulse systems, with high-bit rate data transmission systems.

Acknowledgments

1. E. Yablonovitch and T. J. Gmitter, *Phys. Rev. Lett.* **63** (1989) 1950.

2. J.G. Fleming and Shawn-Yu Lin, *Opt. Lett.* **24** (1999) 49.

3. S. Fan, P.R. Villeneuve, J.D. Joannopoulos, and H.A. Haus, *Phys. Rev. Lett.* **80** (1998) 960.

4. A. D'Orazio, M. De Sario, V. Petruzzelli, and F. Prudenzano, *Opt. Exp*, **11** (2003) 230.

5. S. Kim, I. Park, and H. Lim, *Proc Spie* **5597** (2004) 129.

6. B.E. Nelson *et al.*, *Opt. Lett.* **25** (2000) 1502.

7. M. Koshiba, *J. Lightwave Technol.* **19** (2001) 1970.

8. S.Y. Lin and J.G. Fleming, *J. Lightwave Technol.* **17** (1999) 1944.

9. T.Baba *et al.*, IEEE *J. of Quantum Electron.* **38** (2002) 734.

10. A. D'Orazio, M. De Sario, V. Petruzzelli, and F. Prudenzano, *Opt. Exp.* **11** (2003) 230.

11. U. Peschel *et al.*, *J. Quantum Electronics* **38** (2002) 830.

12. J.A. Besley, J.D. Love, and W. Langer, *J. Lightwave Technology* **16** (1998) 678.

13. B-Sh.Song, T.Asano, Y.Akahane, Y. Tanaka, and S.Noda, *Journal Of Lightwave Technology* **23** (2005) 1449.

14. D.Park, S.Kim, I.Park, and H.Lim, *Journal Of Lightwave Technology* **23** (2005) 1923.

15. Ch. Chen *et al.*, *Opt. Exp.* **13** (2005) 38.

16. S.G. Johnson and J.D. Joannopoulos, *Photonic Crystals: The Road from Theory to Practice* (Kluwer Academic Publishers, 2004).

17. J. Joannopoulos, R.D. Meade, and J.N. Winn, *Photonic Crystals: Molding the flow of light* (Princeton Univers. Press, NJ, 1995).

18. J.P. Berenger, *Phys. Lev. A* **51** (1995) 1571.

19. A. Tavlove, *Computational Electrodynamics*, "The Finite-Difference Time-Domain Method" (Artech House, Norwood, MA, 1995).

20. K.S. Yee, IEEE *Trans. Antennas Propagat.* **AP-14** (1966) 302.